

## Search for DCC in relativistic heavy-ion collisions : Possibilities and Limitations

B. Mohanty<sup>1\*</sup>, T.K. Nayak<sup>1</sup>, D.P. Mahapatra<sup>2</sup> and Y.P. Viyogi<sup>1</sup>

<sup>1</sup>*Variable Energy Cyclotron Centre, Kolkata, 700-064 India*

<sup>2</sup>*Institute of Physics, Bhubaneswar, 751-005 India*

The experimental observation of disoriented chiral condensate is affected due to various physical and detector related effects. We study and quantify the strength of the experimental signal, “neutral pion fraction” within the framework of a simple DCC model, using the analysis methods based on the multi-resolution discrete wavelet technique and by evaluating the signal to background ratio. The scope and limitations of DCC search in heavy-ion collision experiments using various combination of detector systems are investigated.

PACS-key : 25.75.Gz,13.40.-f and Heavy-ion collisions, Disoriented chiral condensates

### 1. Introduction

Disoriented chiral condensates (DCC), localized in phase space, have been predicted to be formed in high energy heavy-ion collisions when the chiral symmetry is restored at high temperatures <sup>1</sup>. The formation of DCC leads to large event-by-event fluctuation in the neutral pion fraction ( $f$ ), defined as

$$f = N_{\pi^0}/N_{\pi} \quad (1)$$

where  $N_{\pi^0}$  and  $N_{\pi}$  are multiplicities of neutral and total pions respectively. The probability distribution of  $f$  inside a DCC domain is given by <sup>2,3</sup>

$$P(f) = \frac{1}{2\sqrt{f}} \quad (2)$$

For normal events the distribution of  $f$  is a binomial peaking at  $\frac{1}{3}$ . The formation of DCC domains gives rise to pion multiplicity fluctuations resulting in the neutral pion fraction deviating significantly from  $\frac{1}{3}$ . Experimentally  $\pi^0$  is detected by its decay product which are photons. Since most of the charged particles detected in an event are charged pions and similarly majority of the photons originate from  $\pi^0$  decay, DCC formation would thus lead to event-by-event correlated fluctuations in the number of charged particles and photons in a given phase space.

Many experiments have attempted to look for DCC and several others are coming up. Experiments so far carried out are based on both cosmic ray studies and

---

\*Corresponding author, e-mail: bmohanty@veccal.ernet.in

accelerators for colliding hadrons and heavy-ions at high energy. The JACEE collaboration had reported the occurrence of a typical anti-CENTAURO event (high  $f$  values) <sup>4</sup>. The mountain top experiments, carried out at Mt. Chacaltaya in Bolivia and Mt. Fuji in Japan, had reported CENTAURO type events (low  $f$  values) <sup>4</sup>. Recently there have been encouraging results from other cosmic ray experiments at Pamir <sup>5</sup>. In the accelerator based experiments, UA1 <sup>6</sup> and UA5 <sup>7</sup>, have done extensive searches for CENTAURO events at the CERN-SPS ( $\bar{p}p$ ) collider. However no indication of CENTAURO events was observed up to  $\sqrt{s} = 900$  GeV. D0 <sup>8</sup>, CDF <sup>9</sup> and Minimax <sup>10</sup> experiments at Fermilab have reported null results. The WA98 <sup>11</sup> and NA49 <sup>12</sup> heavy-ion experiments at CERN-SPS have reported upper limits on DCC production at SPS. While the analysis of the WA98 experiment was based on a systematic study of photon and charged particle multiplicity correlation using the data from a preshower photon multiplicity detector (PMD) and a silicon pad multiplicity detector (SPMD) for charged particles, the NA49 experiment tried to obtain the limits on DCC-type fluctuations based on information from charged particles only.

There now exist many powerful analysis techniques to look for DCC, based essentially on the study of fluctuation in the multiplicity of charged particles and photons <sup>10,11,13,14,15,16</sup>. However, the absence of a reliable dynamical DCC model and the lack of information on various factors affecting the observation of DCC (such as the probability of occurrence of DCC in a reaction at a particular energy, number of possible DCC domains in an event, size of the domains, number of pions emitted from the domains and the interaction of the DCC pions with the rest of the system <sup>1,17,18,19</sup>) make experimental search of domains of DCC difficult. In a recent theoretical study <sup>20</sup>, within the limitations of a simple model of DCC, the probability of formation of DCC at SPS has been predicted to be of the order of  $10^{-3}$  which is close to the upper limit set by an involved analysis of the WA98 data <sup>11</sup>.

For all these experimental techniques to succeed in detecting the DCC signal with very low probability of occurrence, it is necessary to understand, from an experimental point of view, all the factors that affect the detection of DCC domain during its transition from the time of formation to the time of detection. We study this transition by the help of a simple DCC model. The analysis is carried out using the method based on discrete wavelet transformation (DWT) and looking at the signal to background ratio.

Possible factors that affect the DCC signal are : the presence of multiple domains of DCC,  $\pi^0$  decay, increasing particle multiplicity as we go from SPS to RHIC and LHC energies, and the detector related effects, such as efficiency and purity of particle detection and use (or lack) of  $p_T$  information of the detected particles. All these effects are discussed in this paper. This is important from the point of view that the current and future heavy-ion experiments at RHIC and LHC have kept DCC search high on their agenda. At RHIC, STAR experiment plans to look for DCC using the combination of photon multiplicity detector (PMD) and the electromagnetic

calorimeter (EMCAL) for photon detection along with the time projection chamber (TPC) and forward time projection chamber (FTPC) for charged particle detection<sup>21</sup>. The PHENIX experiment has also demonstrated their capability to study isospin fluctuations, essentially through charged particle measurements<sup>22</sup>. At LHC, the ALICE experiment will have the combination of a PMD and a forward charged particle multiplicity detector (FMD) as well as an electromagnetic calorimeter (PHOS) with the time projection chamber (TPC) in a different rapidity region for such a study<sup>23</sup>. In the present article we concentrate on the possibilities and limitations of searching for DCC in experiments using the measurement of charge-to-neutral ratio where the neutral particle (photons primarily from  $\pi^0$  decay) is handled using a preshower detector. We will also briefly discuss other detector combinations.

The paper is organized as follows. In the next section we discuss a simple model of DCC and the methods of analysis used for the present study. In the subsequent sections we discuss the various factors that affect the DCC search using the discrete wavelet transformation technique (DWT). In Section 5 we present the results on the signal to background ratio. Finally we summarize with a discussion on the various limitations and possibilities for DCC search in heavy-ion collisions.

## 2. DCC model and method of analysis

### 2.1. DCC model and simulated events

In the absence of a reliable dynamical model where the effect of the formation of DCC could be simulated at an early stage of the reaction, we take a simple DCC model where the generic particle production is governed by the VENUS event generator<sup>24</sup> and the DCC pions are introduced at the freeze-out stage. The goal is to observe the effect of DCC domains on the measured quantities, assuming DCC pions survive till the freeze-out time. This assumption is justified by the recent calculations<sup>25</sup>.

The following are the main features of the model.

1. DCC-type fluctuations : For DCC simulation in a given domain, the identity of charged pions taken pairwise is changed to neutral ones and vice-versa<sup>11,14</sup>, following the DCC probability as given by Eqn. (2).
2. Domain size : The size of a domain is defined in terms of its extent in pseudo-rapidity ( $\eta$ ) and azimuthal angle ( $\phi$ ). We have chosen a DCC domain with  $\Delta\eta = 1$  and then varied the extent in  $\phi$  (denoted as  $\Delta\phi$ ) to see the effect on observed quantities.
3. Number and  $p_T$  spectrum of DCC pions : For simplicity all the pions inside a chosen domain are considered to be DCC-type. There are theoretical calculations which suggest that DCC pions may have low  $p_T$  and DCC formation may lead to enhancement in the production of low  $p_T$  pions<sup>26</sup>. In order to study the usefulness of  $p_T$  information of particles, we consider two cases - (a)

only pions with  $p_T$  ( $\leq 150$  MeV) are DCC pions in a given domain, and (b) a number of pions (depending on the domain volume) of  $p_T \leq 150$  MeV having DCC origin are added to the generic sample of pions in a given domain.

4.  $\pi^0$  decay and photon fraction : After introducing DCC-type fluctuations the  $\pi^0$ 's are allowed to decay. The neutral pion fraction then gets modified to *photon fraction* given as,

$$f' = (N_\gamma/2)/(N_\gamma/2 + N_{\pi^\pm}) \quad (3)$$

where  $N_\gamma$  is the photon multiplicity and  $N_{\pi^\pm}$  is the total multiplicity of charged pions.

5. Percentage of events being DCC-type : The sets of events with DCC will be referred to as “nDCC” events. The ensemble of nDCC events may or may not have all the events of DCC type. nDCC event ensembles with varying percentage of DCC-type events were generated to study the sensitivity of various physical and detector related effect to the observation of DCC.

## 2.2. Charged particle and photon multiplicity detectors

We assume a hypothetical photon detector placed in the forward region and covering full azimuth in one unit of pseudo-rapidity. The detected photon sample has some admixture of charged particles due to the limitations of photon-hadron discrimination algorithm. The relation between the number of photons incident on the detector ( $N_\gamma$ ) and the number of identified photon-like candidates ( $N_{\gamma\text{-like}}$ ) is given by <sup>27</sup>

$$N_{\gamma\text{-like}} = \epsilon N_\gamma / p \quad (4)$$

where  $\epsilon$  is the photon counting efficiency and  $p$  is the purity of the detected photon sample.

For the present study the photon detector is assumed to have realistic photon counting efficiency of  $70\% \pm 5\%$  and purity of photon sample of  $70\% \pm 5\%$  <sup>28,29,30,31</sup>. The efficiency and purity values are varied to study the role of detector limitation in the observation of DCC.

The charged particles are detected using a hypothetical charged particle detector with an efficiency of  $90\% \pm 5\%$  <sup>32,33</sup>. It is assumed that there is no contamination in the detected charged particle sample (the effect of  $\delta$ -rays are ignored). The charged particle detector is assumed to have complete overlap with the photon detector in  $\eta - \phi$  coverage.

For this work it is assumed that the DCC domain has a complete overlap with the detectors. It may be mentioned that it is not easy to experimentally measure the DCC domain size, if it has been formed in the reaction. It is also difficult to find out experimentally whether the DCC domain formed has a full or partial overlap with the detectors.

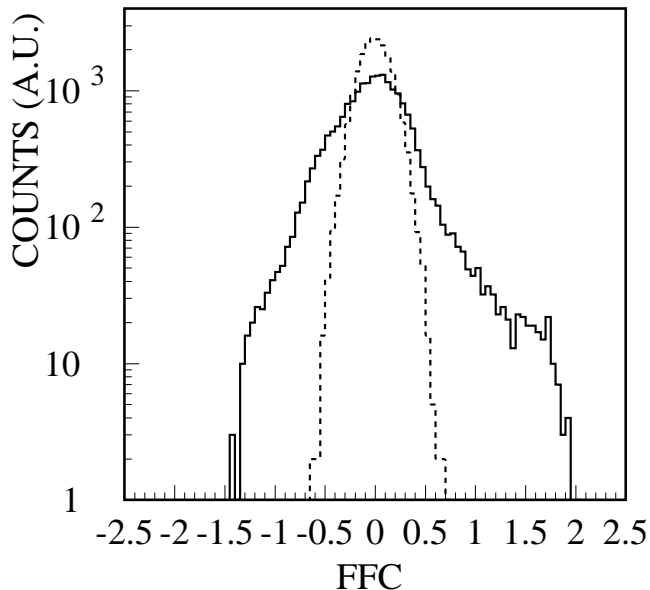


Figure 1: FFC distribution for simulated generic VENUS (dotted line) and pure DCC-like events (solid line). The rms deviation of FFC distribution for DCC-like events is wider than those for VENUS events.

### 2.3. Discrete Wavelet method

Multi-resolution discrete wavelet technique (DWT) has been used to look for bin-to-bin fluctuations in charged particle and photon multiplicity distributions of the simulated events <sup>11,14,34</sup>. The DWT technique has the beauty of analyzing a distribution of particles at different length scales with the ability of finally picking up the right scale at which there is a fluctuation. This method has been utilized very successfully in many fields including image processing, data compression, turbulence, human vision, radar and earthquake prediction. This technique has been suitably adopted here to search for bin to bin fluctuation in the charged particle and photon multiplicity distributions.

The analysis has been carried out by making  $2^j$  bins in  $\phi$  where  $j$  is the resolution scale. The input to the DWT analysis is a sample distribution function given by Eqn. 3 at the highest resolution scale,  $j_{max}$ . The analysis has been carried out using the D-4 wavelet basis <sup>35</sup>. It may be mentioned that there are several families of wavelet bases distinguished by the number of coefficients and the level of iteration; we have used the frequently employed D-4 wavelet basis <sup>35,36</sup>.

The output of the DWT analysis consists of a set of wavelet or father function

coefficients (FFC's) at each scale,  $j = 1, \dots, (j_{max} - 1)$ . It is these FFC's at a given scale that carry information of fluctuation at higher scales. All the analysis have been carried out by taking  $j_{max} = 5$ . Due to the completeness and orthogonality of the DWT basis, there is no information loss at any scale.

The FFC distribution of normal events is a Gaussian while the distribution for events having DCC-type fluctuations has non-Gaussian shapes<sup>11,13,14</sup>. In Fig. 1 we show the typical FFC distribution for pure generic and pure DCC-like events at scale  $j = 1$ . The DCC-like events have a DCC domain of  $\Delta\phi = 90^\circ$  in all events. We find that the FFC distribution for DCC-like events is broader in comparison to that for generic events. The amount of broadening depends on various features associated with DCC domains, In fact, one can show that there is pile up of a large number of events within the width of the generic distribution with decrease in the fraction of DCC-like events.

For comparison of these distributions we use the root mean square (rms) deviations instead of the usual standard deviation. A direct comparison of the rms deviation of FFC distributions for different cases will yield information about the fluctuations. To quantify this effect properly, we define a quantity called strength of DCC signal ( $\zeta$ ) as,

$$\zeta = \frac{\sqrt{(s_X^2 - s_N^2)}}{s_N} \quad (5)$$

where  $s_N$  is the rms deviation of the FFC distribution for normal event set and  $s_X$  is the rms deviation for the different nDCC event sets. The quantity  $\zeta$  also reflects the detectability of the DCC signal. The statistical error on  $\zeta$  has been calculated by varying the number of events and it was found to be  $\sim 0.1$  for the case when all pions in a domain are DCC pions.

#### 2.4. *Signal and Background of DCC events*

In a generic particle production mechanism, because of isospin conservation in strong interaction, the production of  $\pi^0$ ,  $\pi^+$  and  $\pi^-$ , are equally probable. This mechanism leads to a binomial distribution of neutral pion fraction ( $f$ ) peaking at  $\frac{1}{3}$ . For a large number of events having high multiplicity of pions produced, as in heavy-ion collisions, this distribution for normal events can be approximated as a Gaussian with mean at  $\frac{1}{3}$ . Fig. (2) displays the  $f$  distribution of pure DCC events and pure generic events. Since the DCC events lying in the overlap region of the two distributions are difficult to separate, it may be advisable in some analysis to exclude a region around the generic peak. We define :

- Signal (S) = Number of events beyond  $f = f_N^{peak} \pm 2\sigma_N$  in  $f$  distribution of DCC sample,
- Background (B) = The number of events beyond  $f = f_N^{peak} \pm 2\sigma_N$  in the  $f$  distribution of normal sample,

where,  $f_N^{peak}$  is the peak value and  $\sigma_N$  is the standard deviation of the  $f$  distribution of normal events respectively.

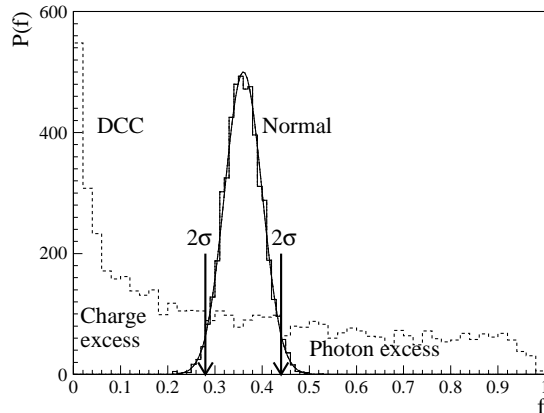


Figure 2: Schematic diagram of the  $f$  distribution of DCC events (dashed lines) and the normal Gaussian distribution of generic events (solid line) peaking at  $1/3$ . Also shown are the regions of photon excess and charge excess and the region within to  $2\sigma$  of the normal distribution.

Here we separately consider the signal in two regions : *charge – excess* events in the left part and *photon – excess* events in the right part of the Fig. (2).

With the analysis methods mentioned we now study the various factors that affect the DCC signal.

### 3. Physical effects

#### 3.1. Effect of Multiplicity

The effect of higher multiplicity is to reduce the event-by-event statistical fluctuation associated with the multiplicity of photons and charged particles. A simple estimate of strength of DCC-type fluctuation shows that for a DCC domain of  $\Delta\phi = 90^\circ$  and  $\Delta\eta$  of one unit, the strength of DCC signal increases with increase in average multiplicity of photons and charged particles. Fig. (3) shows the variation of strength ( $\zeta$ ) of DCC signal with multiplicity, where  $N$  is the average of the mean number of photon and mean number of charged particles in a set of events for one unit in  $\eta$ . One observes that the increase is almost like a  $\sqrt{N}$  effect. This is probably a consequence of going from a narrow Gaussian distribution to a wider  $1/2\sqrt{f}$  distribution. It may be mentioned that typical values of  $N$  in central collisions for  $\Delta\eta \sim 1$ , for the WA98 experiment at SPS (combination of PMD and SPMD detector for charged particle detection) was 320, for STAR (PMD + FTPC) will be about 500 and ALICE (PMD + FMD) will be about 2800 (for an assumed pseudo-rapidity density of  $\sim 8000$  at mid rapidity).

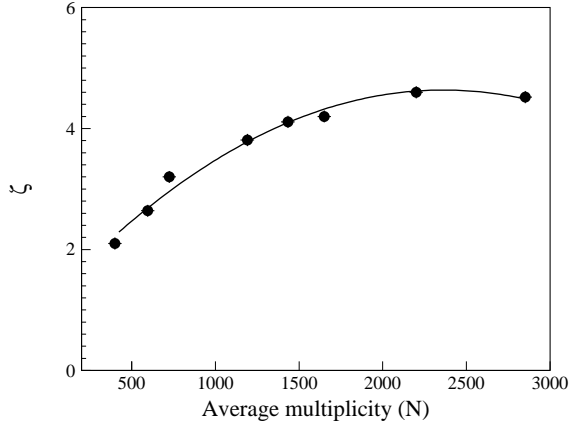


Figure 3: Variation in the strength of DCC signal with multiplicity in a domain of  $\Delta\phi = 90^\circ$  and  $\Delta\eta = 1$ .  $N$  is the average of the sum of mean photon and mean charged particles in a set of events. All the events are DCC events. The solid line is proportional to  $\sqrt{N}$ .

### 3.2. Effect of $\pi^0$ decay

The formation of DCC leads to large event-by-event fluctuation in neutral pion fraction ( $f$ ). To observe this in an ideal situation one has to count the  $\pi^0$ 's event-by-event. But the  $\pi^0$ 's decay into photons by the time they reach the detector.

As a result of decay, photons coming from DCC  $\pi^0$ 's inside a given DCC domain may move out of the domain (depending on the momentum) before they are detected. Also photons from outside the DCC domain will enter the  $\eta - \phi$  phase space of the domain. Both these effects will result in dilution of the strength of the signal. Considering the effect of  $\pi^0$  decay, we modify Eqn. (3) as -

$$f'' = (N_\gamma/2 \pm \delta_\gamma)/(N_\gamma/2 \pm \delta_\gamma + N_{\text{ch}}), \quad (6)$$

where  $\delta_\gamma$  is the resultant number of photons that get removed from or added into the DCC domain and  $N_{\text{ch}}$  is the total number of charged pions. For multiplicity detectors (e.g SPMD in WA98, FMD in ALICE) which do not have the capability of particle identification,  $N_{\text{ch}}$  denotes the multiplicity of all charged particles.

Since  $\delta_\gamma$  is a non zero number, the possibility of observing a pure CENTAURO type event (small  $f$ ) is low. In fact there will be a shift in the  $f''$  away from zero. Fig. (4) shows the original and modified probability distributions  $f$  and  $f''$  inside a DCC domain in the model calculation. Here  $N_{\text{ch}}$  is only  $N_{\pi^\pm}$ , the effect of detecting other charged particles along with pions will be discussed later. Clearly one can notice the shift away from 0 to 0.1 in  $f$  values as a result of decay of  $\pi^0$ 's. Also shown in the figure is the  $f$  distribution for normal events. For normal events  $f$  and



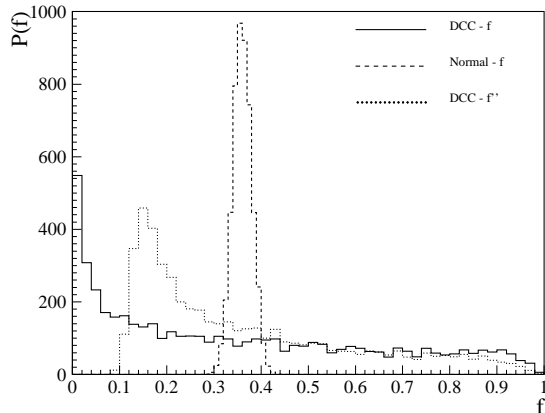


Figure 4: Typical  $f$  distributions inside a DCC domain before (solid line) and after decay (dotted line) of  $\pi^0$  ( $f''$ ). Also shown for comparison is the  $f$  distribution for normal events (dashed line).

$f''$  distributions are not very different because the relative population of  $\pi^0$  is the same within and outside the domain and hence the loss due to decay is compensated by the gain due to decay.

In order to quantify the decrease in the detectability of DCC signal, we consider the following two cases.

(a) Analysis using a  $\pi^0$  detector

In the first case we put two hypothetical detectors, one for detecting  $\pi^0$  and other for detecting charged pions with 100% efficiency within one unit of  $\eta$  and full  $\phi$  coverage. The detector effects will be studied later taking realistic efficiency and other parameters. The goal here is to study the  $\pi^0$  decay effect only. Then we introduce DCC domains with domain size  $\Delta\phi$  varying from  $30^\circ$  to  $180^\circ$ . Thus set of events for a particular DCC domain size are obtained. These events (without  $\pi^0$  decay) and having DCC domain are then analyzed using the DWT method to obtain the FFC distribution. The strength parameter ( $\zeta$ ) is calculated from Eqn. (5), with  $s_X$  corresponding to the rms deviations of the FFC distributions of DCC-type events.

(b) Analysis using an ideal photon detector

In the second case we replace the  $\pi^0$  detector with an ideal photon detector having 100% photon detection efficiency and no contamination of charged particles.

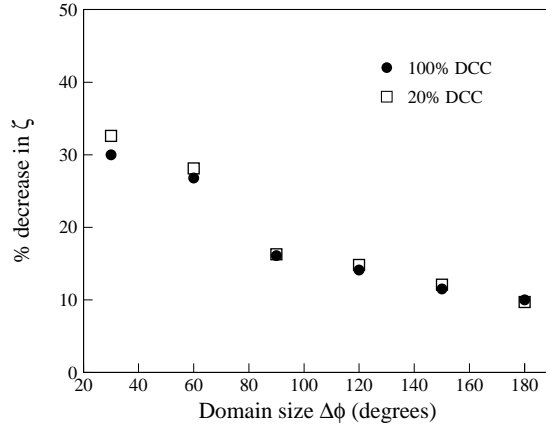


Figure 5: Percentage (%) decrease in the strength of DCC signal due to the effect of decay of  $\pi^0$  as a function of domain size  $\Delta\phi$ .

The  $\pi^0$ 's are allowed to decay. Then we carry out a similar analysis as mentioned above to obtain the strength values.

From the two strength values for each DCC domain size, we calculate the percentage (%) decrease in strength value of the second case compared to the first case. Fig. (5) shows the % decrease in strength of DCC signal due to decay effect for various domain sizes in  $\Delta\phi$ . The results show that the decrease in strength of the signal is more for smaller domains of DCC in comparison to the larger domains.

For each DCC domain size, two cases have been studied : (a) all the events have DCC-type fluctuations and (b) 20% of the events have DCC-type fluctuations introduced. This is done to see the effect of number of events being DCC-type. We find that the results are similar for both 100% and 20% of events being DCC type.

### 3.3. *Effect of multiple domains of DCC*

In heavy-ion collisions there is a possibility that more than one domain of DCC will be formed with chiral condensate pointing in independent direction for each of the domain. It may be mentioned that the precise dimension of a DCC domain is still under debate <sup>26</sup>. In earlier theoretical calculations <sup>37</sup> it has been shown that the DCC signal approaches toward pure normal case with increase in number of domains. In case of multiple domains, the observed neutral pion fraction  $f$ , which is predicted to follow Eqn. (2) for a single DCC domain, will tend toward Gaussian as per the central limit theorem. This makes the dis-entanglement of DCC signal from that of normal events difficult. Subsequent calculations <sup>38</sup> suggest that the situation is better for multiple domains provided one of the domains is predominant.

Here we attempt to quantify the effect of presence of multiple domains with

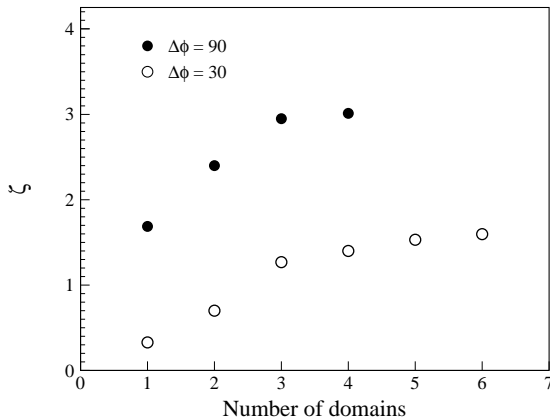


Figure 6: Variation of the strength of DCC signal with increase in number of DCC domains in an event. All the events are DCC events.

the help of the DCC model described earlier and using the multi-resolution DWT method. For simplicity and in view of limitations of the model in terms of introducing DCC at the freeze-out stage, we have placed varying number of DCC domains in an event depending on the domain size in  $\Delta\phi$ . All the domains are assumed to extend 1 unit in pseudo-rapidity. For example, we can place a maximum of four domains of  $\Delta\phi = 90^\circ$ , without any overlap among themselves. We have also carried out the analysis by placing upto six DCC domains in an event with  $\Delta\phi = 30^\circ$ . Care is taken in placing the domains randomly so that no two domains overlap. The  $f$  value of each domain in an event is randomly chosen following the probability distribution given in Eqn. 2. The aim is to see how the signal changes in terms of the strength parameter as given in Eqn. (5).

Fig. (6) shows the variation of strength of DCC signal with number of domains in an event for two domain size of  $\Delta\phi = 90^\circ$  and  $30^\circ$ . We observe that the strength of the DCC signal increases as the number of domains increases and starts saturating for larger number of domains. The increase in strength value with increase in number of domains is because the multi-resolution event-by-event analysis based on DWT method has been able to pick up signals by looking at bin to bin (in  $\phi$ ) fluctuations in each event.

This result is not in contradiction with earlier theoretical observations<sup>37,38</sup>. If the multiple DCC domains formed in the initial stages, in the course of their evolution, move towards the same part of phase space covered by a detector, then the strength of the signal will reduce. However if the phase space separation is maintained in evolving DCC domains, then the strength will increase as found in the present analysis.

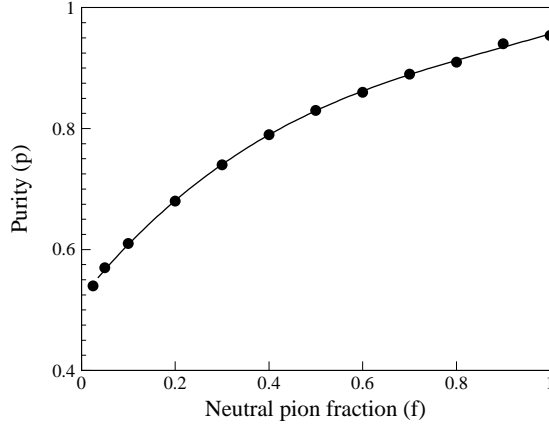


Figure 7: Variation of purity of the photon sample as a function of neutral pion fraction. For  $f = 0.33$  (generic event) purity is  $\sim 0.74$ .

#### 4. Effects due to detector limitations

The detector limitations are basically those related to efficiency and purity of particle detection and the acceptance in  $(\eta, \phi)$ . The effect of efficiency of particle detection is trivial, higher the efficiency of particle detection, more reliable is the search for DCC. Similarly the role of higher acceptance in  $\eta$  and full azimuthal coverage can be hardly over emphasized (lower acceptance effectively reduces the total multiplicity of observable DCC pions and hence reduces the strength of the DCC signal). If the acceptance in  $\eta$  is sizable, one can attempt DWT analysis using bins in  $\eta$  for limited azimuthal coverage, which will be complementary to the present analysis.

The purity of the photon sample, as measured in a detector like PMD, is around 60% – 70%, whereas that of charged particle samples measured using detectors like FTPC or FMD is quite high ( $\geq 95\%$ ). Hence we discuss here only the effect of purity of photon sample.

##### 4.1. *Effect of neutral pion fraction on the purity of photon sample*

It is of interest to study the effect of the DCC neutral pion fraction on the purity of photon sample. Consider a case where the neutral pion fraction ( $f$ ) for a DCC domain has a value of 1. This corresponds to a case where there are no charged pions. This will lead to greatly reduced number of charged particles falling on the photon detector. So the purity of the photon sample will be high. The variation of purity with neutral pion fraction can be investigated in the following manner.

The number of  $\gamma$  - *like* hits on the photon detector can be written as

$$N_{\gamma\text{-like}} = \epsilon N_{\gamma} + c N_{ch} \quad (7)$$

where the first term denotes the contribution of actual photons and the second term denotes charged particle contamination.  $c$  is the fraction of  $N_{ch}$  on the PMD acceptance treated as contamination to the detected photon sample.

We assume that the fraction  $c$  is given by a normal distribution with mean of 15% and  $\sigma$  of 5%, the percentage being taken with respect to the total charged particles within the acceptance of the photon detector. This is a reasonable number, considering that the converter thickness of the preshower detector is  $\sim 10\%$  of an interaction length and some interactions lead to multiple clusters (the effect of overlapping clusters is ignored). DCC-type fluctuations are introduced for *fixed*  $f$  values and domain size  $\Delta\phi = 360^\circ$  and  $\Delta\eta = 1$  in a set of event. Several such sets of events were generated for  $f$  values varying from 0.025 to 1.0. The purity of photon sample is then calculated for each set of events with a *fixed* neutral pion fraction value.

The results are shown in Fig. (7). One clearly sees that the purity of photon sample increases with the increase in the neutral pion fraction value. However the purity does not reach a value of 1 for  $f = 1$ , because there are charged particle other than  $\pi^\pm$  falling on the detector. Similarly it never reaches a value of zero for  $f = 0$ , as there are  $\gamma$ 's from  $\pi^0$ 's decaying outside the detector acceptance and from other sources.

#### 4.2. Effect of charged particle contamination in PMD

Photon measurement in heavy-ion collisions has the problem of charged particle contamination. The charged particles detected as photons have a correlation with those detected in the charged particle multiplicity detector. This additional correlation suppresses the anti-correlation between the photons and charged particles that arises due to DCC formation.

The effect of such a correlation has been studied with the help of VENUS (no DCC) events and a set of mixed events generated from them. The percentage of charged particle contamination was varied from 0% to 50%. The event-by-event  $N_{\gamma\text{-like}}$  was kept the same for all the cases. The result of the DWT analysis on these events is shown in Fig. (8). There is a decrease in the rms deviation of the FFC distribution for pure VENUS events with increase in the % contamination in the photon sample. Thus presence of any additional anti-correlation due to DCC-like effect will have to overcome the opposing correlation effect due to contamination in order to be observed.

Mixed events form an important tool for comparison with data <sup>11</sup> in order to draw any conclusion regarding the presence of fluctuations. The mixed events were generated by mixing hits in the photon detector and charged particle detector separately from different events and ensuring that no two hits in a mixed event came from the same real event. A realistic two-track resolution was assumed for the two

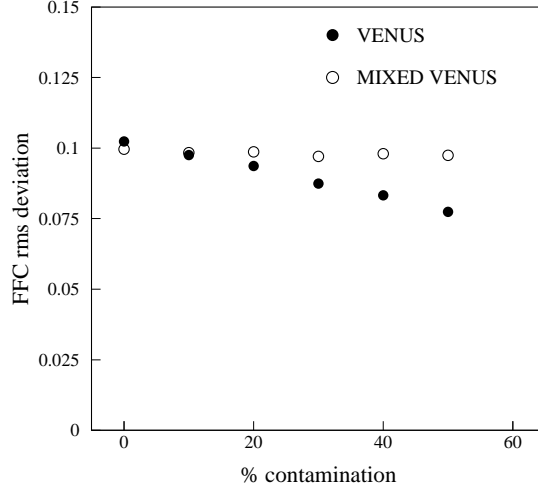


Figure 8: Variation of rms deviation of FFC distribution for pure VENUS events with increase in % of contamination in the photon detector. The variation of rms deviation of FFC distributions of mixed events constructed from VENUS are also shown.

detectors<sup>28,32</sup> and this was taken into account in the event-mixing process. The mixed event  $N_{\gamma\text{-like}}-N_{ch}$  distribution is constructed to be identical to the  $N_{\gamma\text{-like}}-N_{ch}$  distribution of the VENUS events for the full acceptance region of the detectors. This is done by producing one mixed event for each real event with the same multiplicity of  $N_{\gamma\text{-like}}$  and  $N_{ch}$  pair as in the VENUS event. This preserves in detail the  $N_{\gamma\text{-like}}-N_{ch}$  correlation.

Fig. (8) also shows the effect of contamination on mixed events generated from the VENUS events. It is found that the rms deviations of the FFC distributions for the mixed events remain independent of the level of contamination. The mixed events appropriately break the additional correlation due to charged particle contamination.

The effect of charged particle contamination can be corrected by knowing the level of contamination in photons for a given detector. Fig. (9) shows the variation of rms deviation of FFC distribution for DCC-like events with increase in % of events being DCC-type in a given ensemble of nDCC events. It also shows the variation of rms deviation of FFC distribution of corresponding mixed events constructed as described above. The rms deviations of the FFC distribution of mixed events are found to be independent of % of events being DCC-type. This is along the expected lines. But for lower % of events being DCC-type it is above that of the parent sample of nDCC events. This is because the  $N_{\gamma\text{-like}} - N_{ch}$  anti-correlation due to DCC-type effect is not sufficient to overcome the correlation between  $N_{ch}$

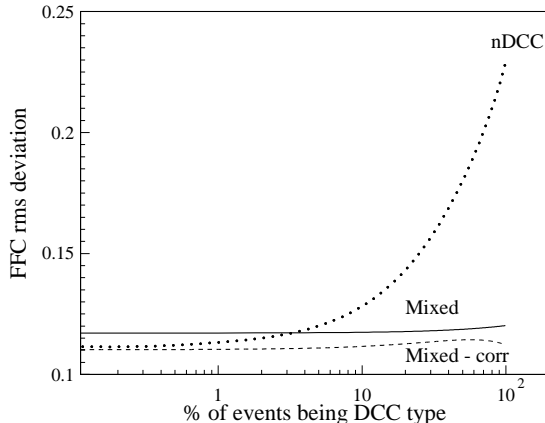


Figure 9: Variation of rms deviation of FFC distribution of DCC-type events as a function of % of events being DCC-type. Also shown are the results for corresponding mixed events and mixed events corrected for contamination effect.

and charged particle detected as contamination in the photon detector. However as the % of events being DCC-type increases, the DCC-type effect dominates. The effect of the contamination can be corrected. This is done by taking into account the difference in rms deviation of normal events and mixed events. The rms deviation of FFC distribution of corrected mixed events are shown in Fig. (9).

The results from above two subsections indicate that it is better to look for anti-CENTAURO (photon excess) events in studies using photon and charged particle multiplicity detectors. This is because, the effect of decay is primarily to shrink the  $f$  distribution from the lower  $f$  side and high value of  $f$  leads to a reduced effect of charged particle contamination on DCC search.

#### 4.3. Effect of $p_T$ information of charged particles and photons

It is expected that  $p_T$  information of particles would be very helpful in DCC search. This would also enable one to verify the various predicted features of DCC formation, such as, DCC-pions are low  $p_T$  pions and DCC formation may lead to low  $p_T$  enhancement in pions <sup>26</sup>.

In order to show the utility of  $p_T$  information we carried out the following study. Here we assume that all charged particles with  $p_T$  greater than 50 MeV/c are detected ( the  $p_T$  acceptance of preshower detector like PMD extends down to 30 MeV/c <sup>28</sup>). The  $p_T$  resolution for the charged particle detector was taken as  $\frac{\Delta p_T}{p_T} = 0.2$  <sup>33</sup>. These realistic parameters are taken from a typical experiment for DCC search, as in STAR. Since DCC pions are believed to have low  $p_T$ , in our simulation we introduce DCC-type fluctuations in pions with  $p_T \leq 150$  MeV/c. Then a DWT

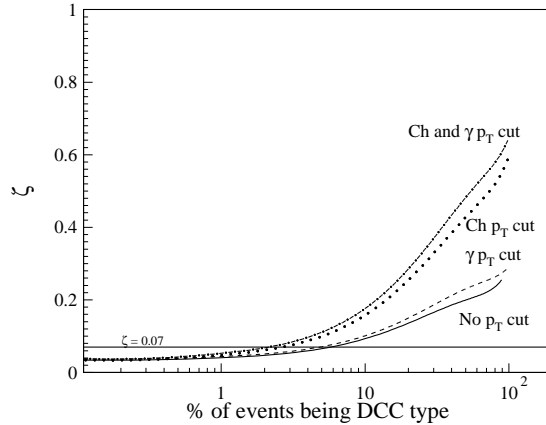


Figure 10: Variation of  $\zeta$  as a function of % of events being DCC-type, for charged particle detector with  $p_T$  information and photon detector without  $p_T$  information (dotted line), for photon detector with  $p_T$  information and charged particle detector without  $p_T$  information (dashed line) and for both charged particle and photon detector with  $p_T$  information (dot-dashed line). Also shown are the corresponding results with both charged particle detector and photon detector without  $p_T$  information (solid line). The horizontal straight line indicates the statistical error on  $\zeta$ .

analysis is carried out. The sample function in the DWT analysis is modified, such that  $N_{\text{ch}}$  taken corresponds to those having  $p_T \leq 150 \text{ MeV}/c$ .

In Fig. (10) we show the strength,  $\zeta$ , of the DCC signal as a function of percentage (%) of events being DCC-type. For comparison also shown is the corresponding  $\zeta$  where the charged particle detector has no  $p_T$  information. We note that the absolute value of  $\zeta$  is lower compared to those presented in previous sections. This is because here we have taken only low  $p_T$  pions as DCC pions in a given domain, whereas earlier all the pions in the domain were considered to be DCC-type. This reduces the strength  $\zeta$  as a result of reduction in multiplicity. The statistical error on  $\zeta$  for the present case is 0.07.

Clearly one can see the increase in strength of the signal with the use of  $p_T$  information. We carry out the same analysis assuming that all photons have  $p_T$  information while the charged particles do not have any  $p_T$  information. The results are also shown in Fig. (10). One finds that although there is an increase in signal strength, it is more for event sample having a larger fraction of DCC events and much less compared to having  $p_T$  information for charged particles. For the case where the analysis is carried out assuming that both photons and charged particles have  $p_T$  information, one finds that the results are close to those obtained for charged particle detector with  $p_T$  information, except for events having higher



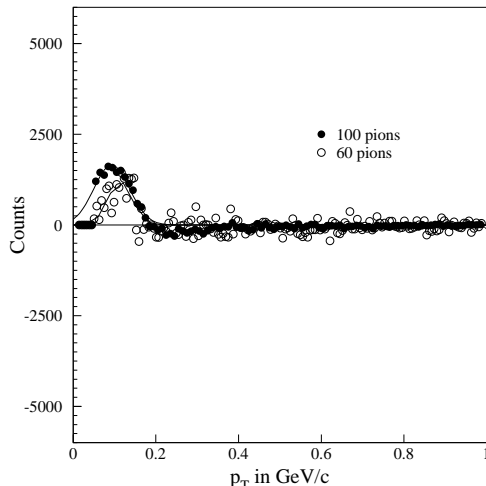


Figure 11: Resultant  $p_T$  distribution of charged particles with 20% of the events being DCC-type, obtained by subtracting the  $p_T$  distribution of charged particles within  $2\sigma$  of the FFC distribution from those beyond. Two cases are presented, additional low  $p_T$  DCC pions being 60 and 100. The statistical errors are within the symbol size.

percentage of DCC type events.

It is also believed that DCC formation may lead to low  $p_T$  enhancement. This hypothesis can be checked if the  $p_T$  of charged particles is measured. In order to incorporate this effect in simulation, a number of low  $p_T$  pions ( $p_T \leq 150$  MeV/c), generated according to DCC probability given in Eqn. (2) and having uniform  $p_T$  distribution were added within the chosen domain on top of the existing pions of a normal event<sup>14</sup>. The number of pions to be added depends on the size of DCC domain and energy density of the domain. Assuming that the energy density within a DCC domain is about  $50$  MeV/ $f m^3$  and domain radius of the order of  $3 - 4$  fm<sup>26</sup> we have performed simulations taking 100 and 60 additional low  $p_T$  pions. As a test case we have taken a sample with 20% of the events having a DCC domain of size  $\Delta\phi = 90^\circ$  and  $\Delta\eta = 1$ .

The event sample is analyzed by the DWT method to obtain the FFC distribution, which was found to be near Gaussian for the present case. We divide the FFC distribution into two parts, (a) one within  $\pm 2\sigma$  of the mean and (b) another beyond this. We obtain the  $p_T$  distributions of the two sets of events. Then we subtract the histogram corresponding to events within  $2\sigma$  of the FFC distribution from those beyond, after proper normalization. The resultant spectrum is shown in Fig. (11).

Clearly one sees that if DCC results in low  $p_T$  enhancement then following the

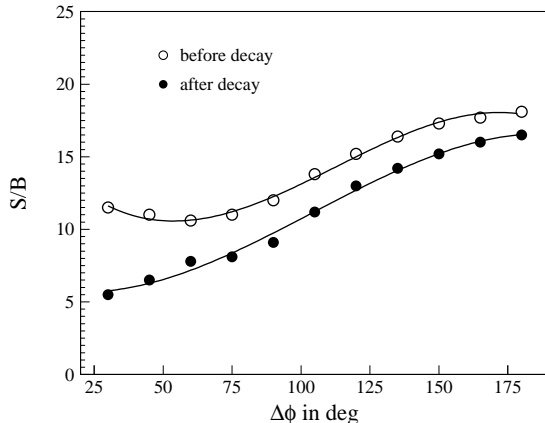


Figure 12: Signal (S) to Background (B) ratio of DCC signal before and after the decay of  $\pi^0$ , as a function of DCC domain size.

above analysis technique in data, one should be able to observe such an effect. The effect is more for case of 100 additional DCC pions compared to case of 60 additional DCC pions.

## 5. Signal and Background of DCC events

The signal to background ratio of DCC events defined in section 2.4 gets modified due to  $\pi^0$  decay (which leads to shrinking of the  $f$  distribution for DCC events) and also due to the effect of charged particle contaminants in the photon detector. In this section we first discuss the effect of  $\pi^0$  decay and then we discuss the effect of various detector effects on the signal to background ratio of DCC events.

An analysis of the events as described in section 2.1, to evaluate the signal to background ratio gives similar results as obtained from the DWT method. Fig. (12) shows the  $S/B$  values before and after decay as a function of size of the DCC domain in azimuth. One clearly observes that the decrease in  $S/B$  value for smaller domains is more compared to that for larger domains.

The efficiency along with the charged particle contamination in photon sample as discussed in previous sections, causes a further shrinkage in the  $f$  values inside a typical DCC domain as shown in Fig. (13). This is in addition to those due to  $\pi^0$  decay shown in Fig. (4). The  $f$  distribution for normal events is now wider.

Signal to background ratio for typical detector parameters are shown in Figs. (14) and (15) as a function of DCC domain size and percentage of events being DCC-type for a given domain size respectively. From Fig. (14) one observes that the  $S/B$  ratio increases with increase in domain size. If one separates the  $S/B$  ratio for photon excess and charge excess events, then one observes that  $S/B$  ratio for

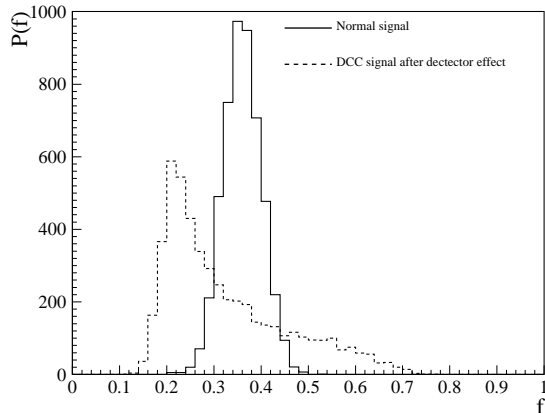


Figure 13: Typical  $f$  distributions inside a DCC domain after detector effects, such as charged particle contamination and realistic efficiency of photon and charged particle detectors. Also shown for comparison is the  $f$  distribution of the corresponding normal events.

photon excess events is larger for smaller DCC domains.

Fig. (15) shows the  $S/B$  ratio as a function of percentage of events being DCC-type for a DCC domain of  $90^\circ$  in azimuth. One observes that the  $S/B$  ratio increases with increase in the number of events being DCC-type. One also notices that the  $S/B$  ratio of photon excess events is much larger than those for charge excess events.

Although these results are along expected lines (the signal increases as the number of DCC pions increases and also as number of events with DCC-type fluctuations increases), it clearly shows that it is more advantageous to look for photon excess events.

## 6. Discussion and Summary

The results presented here describe the limitations and the possibilities of DCC search in heavy-ion collisions. We have discussed various factors that affect the DCC signal (fluctuation in  $f$ ) using a simple DCC model, a multi-resolution analysis technique based on wavelet transformation and an estimation of signal to background ratio.

Among the possibilities, contrary to the theoretical results so far on multiple domains of DCC, we find that these can still be looked for without much loss in signal strength if the domains do not overlap. This is possible through a multi-resolution analysis carried out by binning the  $\eta - \phi$  phase space, as done in the discrete wavelet transformation method. Increase in multiplicity of the particles produced as one goes from SPS to RHIC and LHC energies results in lower statistical

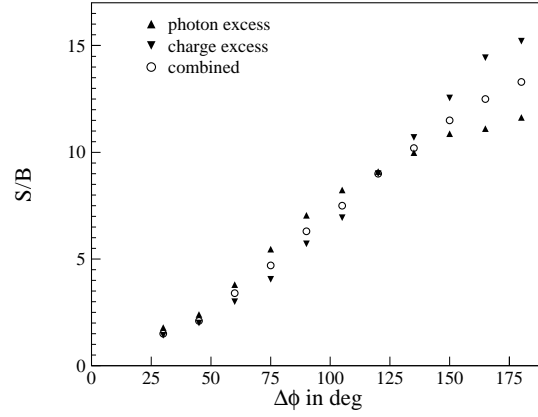


Figure 14: The variation of signal(S) to background (B) ratio as a function of DCC domain size. In the event sample all events are DCC type and the results are obtained after including decay and detector effects. The S/B values for photon excess (higher  $f$  values) and charge excess (lower  $f$  values) cases are also shown.

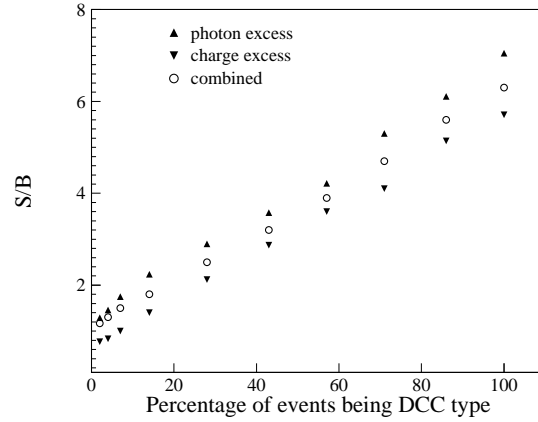


Figure 15: The variation of signal (S) to background (B) ratio as a function of percentage of events being DCC type in a given sample of events. Here the DCC domain chosen is  $90^\circ$  in  $\phi$  and the results are obtained after taking the detector effects into account. The S/B vales for photon excess (higher  $f$  values) and charge excess (lower  $f$  values) cases are also shown.

fluctuations in the observables analyzed. We have also shown that the possibility of DCC search is increased if charged particle detector has  $p_T$  information. However one finds that, primarily due to the decay kinematics of  $\pi^0$  to photons, the effect of photon detector with  $p_T$  information on DCC signal strength is not appreciable. A charged particle detector having  $p_T$  information along with photon multiplicity detector will be a better setup to look for fluctuations in primary signal of DCC, i.e the photon fraction, specially for the anti-CENTAURO type events.

One of the major limitation to the detection of DCC signal is the decay of  $\pi^0$  to photons. It also reduces the possibility for observing low  $f$  (CENTAURO) events. The other major limitation is the correlation arising due charged particle contamination in the photon detector. It reduces the strength of the DCC signal. However, this limitation can be overcome by knowing the amount of charged particle contamination in the photon detector. The purity of photon sample increases for a DCC event with higher  $f$  value. Thus looking for higher  $f$  (anti-CENTAURO) events is advisable.

The other limitations are due to efficiency, granularity and the finite acceptance of the detectors. Reduced acceptance greatly reduces the strength of the DCC signal. Thus DCC studies will be affected using the TPC + PHOS combination in ALICE, even though this combination will be able to provide  $p_T$  information for both photon and charged particles.

One observes that the signal to background ratio for photon excess (anti-CENTAURO) events is higher than those for the charge excess (CENTAURO) events for DCC domains upto  $120^\circ$  in azimuth. And for these domains the S/B ratio for the photon excess events are higher compared to charge excess events as a function of percentage of events being DCC-type. Thus it is advisable to look for photon excess events in an experimental event sample for looking at DCC-type fluctuations, using a photon multiplicity detector and a charged particle multiplicity detector having particle wise  $p_T$  information.

**Acknowledgments :** One of us (B.M.) is grateful to the Board of Research on Nuclear Science of the Department of Atomic Energy, Government of India for financial support in the form of Dr. K.S. Krishnan Fellowship.

1. K. Rajagopal, F. Wilczek, Nucl. Phys. **B399** 395 (1993).
2. J. -P. Blaizot and A. Krzywcki, Phys. Rev. **D46** 246 (1992).
3. J.D. Bjorken, Int. J. Mod. Phys. **A7** 4189 (1992).
4. C.M.G. Lattes, Y. Fujimoto, S. Hasegawa, Phys. Rep. **65** 151 (1980).
5. C.R.A. Augusto et al., Phys. Rev. **D59** 054001 (1999).
6. G. Arnison et al. (UA1 Collaboration), Phys. Lett. **B122** 189 (1983).
7. G.J. Alner et al. (UA5 Collaboration), Phys. Lett. **B180** 415 (1986).
8. M.V.S. Rao (for D0 Collaboration), Fermilab-CONF-94-343-E, Sept 1994.
9. P.L. Melese (for CDF Collaboration), Fermilab-CONF-96-205-E, July 1996.
10. T.C. Brooks et al., (Minimax Collaboration), Phys. Rev. **D61** 032003 (2000).
11. M.M. Aggarwal et al., (WA98 Collaboration), Phys. Rev. **C64**, 011901(R) (2001); eprint : nucl-ex/0206017.
12. H. Appelshausen et al., (NA49 Collaboration), Phys. Lett. **B459** 679 (1999).

13. B.K. Nandi et al., Phys. Lett. **B449** 109 (1999).
14. B.K. Nandi et al., Phys. Lett. **B461** 142 (1999).
15. B. Mohanty et al., Phys. Rev. **C66** 044901 (2002).
16. Bedangadas Mohanty, eprint : nucl-th/0203005, To appear in Int. J. Mod. Phys. A.
17. M. Asakawa et al., Phys.Rev.Lett. **74** 3126 (1995).
18. James Hormuzdiar and Stephen D.H. Hsu, Phys.Rev. **C58** 1165 (1998).
19. Jorgen Randrup and Robert L. Thews, Phys. Rev. **56** 4392 (1997).
20. A. Krzywicki and J. Serreau, Phys. Lett. **B448** 257 (1999); Julien Serreau, Phys.Rev. **D63** 054003 (2001).
21. STAR Contributions to a NIM Volume Dedicated to the Detectors and the Accelerator at RHIC, To be published in Nucl. Instr. and Methods.
22. T. Nakamura (for PHENIX Collaboration), Poster at QM2002 titled “*Study of isospin fluctuations at RHIC-PHENIX*”.
23. ALICE Collaboration, Technical Proposal, CERN/LHCC/95-71 (1995).
24. K. Werner, Phys. Rep. **C232** 87 (1993).
25. James V. Steele and Volker Koch, Phys. Rev. Lett. **81** 4906 (1998).
26. J.I. Kapusta and A.P. Vischer, Z. Phys. **C75** 507 (1997); S. Gavin, A. Goksch and R.D. Pisarski, Phys. Rev. Lett. **72** 2143 (1994).
27. M.M. Aggarwal et al., (WA98 Collaboration), Phys. Lett. **B458** 422 (1999).
28. M.M. Aggarwal et al., Nucl. Instr. and Methods **A424** 395 (1999).
29. A.K. Dubey et al., Photon multiplicity detector – Technical proposal (For STAR Experiment) VECC/EQG/00-04, (2000).
30. M.M. Aggarwal et al., Nucl. Instr. and Methods **A488** 131 (2002); ALICE Collaboration, photon multiplicity detector – ALICE technical design report, (ALICE Collaboration), G. Dellacasa et al., CERN/LHCC 99-32, ALICE TDR 6, 30 September 1999.
31. S. Chattopadhyay et al., Nucl. Instr. and Methods **A421** 558 (1999).
32. W.T. Lin et al., Nucl. Instr. Methods **A389** 415 (1997).
33. STAR FTPC Proposal, MPI-PhE/98-3 (1998).
34. Zheng Huang, Ina Sarcevic, Robert Thews and Xin-Nian Wang, Phys. Rev. **D54** 750 (1996).
35. I. Daubechies, Orthonormal Bases of Compactly Supported Wavelets, Comm. Pure & Appl. Math **41** 909 (1998).
36. Amara Graps, IEEE Comput. Sci. Eng **2** 50 (1995).
37. R.D. Amado and Yang Lu, Phys. Rev. **D54** 7075 (1996).
38. Q.H. Zhang and X.Q. Li, Phys. Rev. **D55** 7302 1997.